IJST (2014) 38A3 (Special issue-Mathematics): 329-336
Iranian Journal of Science & Technology

http://ijsts.shirazu.ac.ir

Adaptive mesh generation for approximation of traffic flow equations

A. R. Soheili[1, 2]* and N. Davoodi[2]

[1]*The Center of Excellence on Modelling and Control Systems, Ferdowsi University of Mashhad, Mashhad, Iran*
[2]*Department of Applied Mathematics, Faculty of Mathematical Sciences,*
Ferdowsi University of Mashhad, Mashhad, Iran
E-mail: soheili@um.ac.ir

Abstract

This paper introduces a mesh generating algorithm for solving the traffic flow equation as a conservation law equation. The idea behind the new method is to use the characteristic curves and moving non-oscillatory finite volume method. In addition, when characteristic curves intersect, the proposed scheme uses shock speed equation in order to improve computational efficiency. We also compare the obtained results with the corresponding solutions computed by the moving mesh method.

Keywords*:* Traffic flow; characteristic curves; shock speed; moving finite volume method

1. Introduction

We propose to investigate traffic phenomena from the macroscopic point of view, using models derived from fluid-dynamics consisting of hyperbolic conservation laws. In recent years, many interesting works have developed in the numerical treatment of PDEs, giving rise to conservation laws and, particularly, the traffic flow equation:

$$\frac{\partial \rho(x,t)}{\partial t} + \frac{\partial F(\rho(x,t))}{\partial x} = 0, \qquad (1)$$

The LWR model (Lighthill and Whitham, 1955; Richards, 1956) is known as a simple continuum model, in which the relationships among three aggregate variables are modeled: traffic density $\rho(x,t)$, flow rate $F(\rho(x,t))$, and space mean speed $u(x,t)$. In this model $F(\rho(x,t)) = \rho u$, while t and x represent time and space, respectively. In the LWR model, the velocity is given by some specific known function $u = u(\rho)$ for $0 \le \rho \le 1$. There are also other higher order models. Examples of such models including the traffic model are given in (Jiang et al., 2002; Payne, 1971; Tang et al, 2010; Zhang, 1998).

In (Jiang et al., 2002), the traffic model is described by the following system of partial differential equation:

$$\begin{cases} \frac{\partial \rho(x,t)}{\partial t} + \frac{\partial F(\rho(x,t),u(x,t))}{\partial x} = 0, \\ \frac{\partial u(x,t)}{\partial t} + \frac{\partial G(u(x,t))}{\partial x} = g(\rho(x,t),u(x,t)), \end{cases} \qquad (2)$$

where $F\big(\rho(x,t),u(x,t)\big) = \rho u$, $G\big(u(x,t)\big) = \frac{u^2}{2} - c_0 u$ and $g(x,t)$ is the generation rate.

In order to efficiently model numerical solution of these equations, it is convenient to resort to an adaptive grid technique that automatically concentrates the spatial nodes in the regions of rapid solution variations (i.e., the wave moving fronts). Several moving mesh techniques have been introduced in the past for solving the problems governed by the hyperbolic conservation laws (Huang et al., 1994; Huang and Russell, 2011; Soheili et al, 2012; Stockie et al., 2001; Tang and Tang, 2003).

In this paper, an adaptive moving mesh algorithm based on the characteristic curves is presented. The following section will briefly describe the coupled equations and the finite-volume formulation used in our computations. The moving mesh algorithm will be discussed in this Section, and several numerical tests will be given in Section 3. We then compare the numerical results of the new method and moving mesh method (MMPDE5) in section 4. Finally, concluding remarks and a summary of findings are given in Section 5.

2. New adaptive numerical method

Our adaptive numerical scheme is based on two independent parts: a mesh-generation algorithm and a numerical solution algorithm. For numerical solution, we use non-oscillatory finite volume method (Godlewski and Raviart, 1996; Leveque, 2002; Nessyahu and Tadmor, 1990) and for mesh-generation, we apply characteristic curves and shock speed of equation.

2.1. Non-oscillatory finite volume method for a system of equations

We begin with a brief description of the Non-oscillatory finite volume schemes used to numerically

*Corresponding author
Received: 5 September 2013 / Accepted: 16 April 2014

solve the equations (1) and (2). The moving Non-oscillatory method that we have just used in the traffic equations (Soheili et al, 2013), can also be applied to a system of equations. However, this method can be extended to a system of equations with the source term:

$$\begin{cases} \frac{\partial \rho(x,t)}{\partial t} + \frac{\partial F(\rho(x,t),u(x,t))}{\partial x} = 0, \\ \frac{\partial u(x,t)}{\partial t} + \frac{\partial G(u(x,t))}{\partial x} = g(\rho(x,t),u(x,t)). \end{cases} \quad (3)$$

Suppose $x_j^n = x_{min} + (j-\frac{1}{2})\Delta x_{j,}^n\ t_n = t_{n-1} + \Delta t_n$, where Δx_n^j, Δt_n are small spatial and temporal scales around the time $t = t_n$.
Let

$$[x_{min}, x_{max}] = \bigcup_{j=1}^{N} C_j^n, \quad C_j^n = [x_{j-\frac{1}{2}}^n, x_{j+\frac{1}{2}}^n].$$

The value $\bar{u}_j^n$ will approximate the average value over the jth cell C_j at time t_n:

$$\bar{\rho}_j^n = \frac{1}{\Delta x_j^n}\int_{C_j^n} \rho(x,t_n)dx, \quad (4a)$$

$$\bar{u}_j^n = \frac{1}{\Delta x_j^n}\int_{C_j^n} u(x,t_n)dx, \quad (4b)$$

where $\Delta x_j^n = x_{j+\frac{1}{2}}^n - x_{j-\frac{1}{2}}^n$ is the length of the j-th cell.
We then construct its piecewise linear interpolant

$$\tilde{\rho}^n(x) = \bar{\rho}_j^n + w_j^n(x - x_j^n),\ x \in C_j^n, \quad (5a)$$

$$\tilde{u}^n(x) = \bar{u}_j^n + s_j^n(x - x_j^n),\quad x \in C_j^n. \quad (5b)$$

The slopes w_j^n, s_j^n are first-order approximations of $\rho_x(x_j^n, t_n)$, $u_x(x_j^n, t_n)$. Here, we have used the generalized minmod reconstruction with

$$w_j^n = minmod\left(\theta\frac{\bar{\rho}_j^n - \bar{\rho}_{j-1}^n}{x_j^n - x_{j-1}^n}, \frac{\bar{\rho}_{j+1}^n - \bar{\rho}_{j-1}^n}{x_{j+1}^n - x_{j-1}^n}, \theta\frac{\bar{\rho}_{j+1}^n - \bar{\rho}_j^n}{x_{j+1}^n - x_j^n}\right),\ \theta \in [1,2], \quad (6)$$

$$s_j^n = minmod\left(\theta\frac{\bar{u}_j^n - \bar{u}_{j-1}^n}{x_j^n - x_{j-1}^n}, \frac{\bar{u}_{j+1}^n - \bar{u}_{j-1}^n}{x_{j+1}^n - x_{j-1}^n}, \theta\frac{\bar{u}_{j+1}^n - \bar{u}_j^n}{x_{j+1}^n - x_j^n}\right),\ \theta \in [1,2], \quad (7)$$

where $\theta = 2$ has been chosen.
Integrating (3) over $[x_j^n, x_{j+1}^n] \times [t_n, t_{n+1}]$ yields

$$\bar{\rho}_{j+\frac{1}{2}}^{n+1} = \frac{1}{\Delta x_j^n}\int_{x_j^n}^{x_{j+1}^n} \tilde{\rho}^n(x)dx - \frac{1}{\Delta x_j^n}\int_{t_n}^{t_{n+1}} [F\left(\rho(x_{j+1}^n, t)\right) - F(\rho(x_j^n, t))]dt, \quad (8)$$

and

$$\bar{u}_{j+\frac{1}{2}}^{n+1} = \frac{1}{\Delta x_j^n}\int_{x_j^n}^{x_{j+1}^n} \tilde{u}^n(x)dx - \frac{1}{\Delta x_j^n}\int_{t_n}^{t_{n+1}} [F(u(x_{j+1}^n, t)) - F(u(x_j^n, t))]dt + \int_{t_n}^{t_{n+1}}\int_{x_j^n}^{x_{j+1}^n} g(\rho(x,t),u(x,t))dxdt. \quad (9)$$

In a method with changing mesh widths, the stability criterion for the time step is more important. It is essential to note that the CFL condition is only a *necessary* condition for stability (and hence convergence). The standard CFL limit reads (Leveque, 2002)

$$|F_\rho\frac{\Delta t}{\Delta x}| \le 1, \quad |G_u\frac{\Delta t}{\Delta x}| \le 1, \quad \forall\, \Delta x, \Delta t.$$

To enforce higher accuracy, the Courant number will here be limited by a parameter $\mathcal{C}$, thereby limiting the time step to:

$$\Delta t_n \le \mathcal{C}\min_j\left\{\frac{\Delta x_j^n}{|F_\rho(\bar{\rho}_j^n)|}, \frac{\Delta x_j^n}{|G_u(\bar{u}_j^n)|}\right\} = \mathcal{C}\min_j\left\{\frac{\Delta x_j^n}{|\lambda_1(x_j^n)|}, \frac{\Delta x_j^n}{|\lambda_2(x_j^n)|}\right\},$$

Where $0 < \mathcal{C} < 1$ and $\lambda_1(x_j^n), \lambda_2(x_j^n)$ are the eigenvalues of the Jacobian matrix of the flux function F.

Therefore, the flux integrals in (8) and (9) can be safely approximated by the mid-point quadrature leading to

$$\bar{\rho}_{j+\frac{1}{2}}^{n+1} = \frac{1}{\Delta x_{j+\frac{1}{2}}^n}\Big[(x_{j+\frac{1}{2}}^n - x_j^n)\rho_j + (x_{j+1}^n - x_{j+\frac{1}{2}}^n)\rho_{j+1} + \frac{w_j}{2}(x_{j+\frac{1}{2}}^n - x_j^n)^2 - \frac{w_{j+1}}{2}(x_{j+\frac{1}{2}}^n - x_{j+1}^n)^2\Big] - \frac{\Delta t_n}{\Delta x_{j+\frac{1}{2}}^n}\Big[F(\rho(x_{j+1}^n, t^{n+\frac{1}{2}})) - F(\rho(x_j^n, t^{n+\frac{1}{2}}))\Big], \quad (10a)$$

$$\bar{u}_{j+\frac{1}{2}}^{n+1} = \frac{1}{\Delta x_{j+\frac{1}{2}}^n}\Big[(x_{j+\frac{1}{2}}^n - x_j^n)u_j + (x_{j+1}^n - x_{j+\frac{1}{2}}^n)u_{j+1} + \frac{s_j}{2}(x_{j+\frac{1}{2}}^n - x_j^n)^2 - \frac{s_{j+1}}{2}(x_{j+\frac{1}{2}}^n - x_{j+1}^n)^2\Big] - \frac{\Delta t_n}{\Delta x_{j+\frac{1}{2}}^n}\Big[G(u(x_{j+1}^n, t^{n+\frac{1}{2}})) - G(u(x_j^n, t^{n+\frac{1}{2}}))\Big] + \frac{1}{\Delta x_{j+\frac{1}{2}}^n}\int_{t_n}^{t_{n+1}}\int_{x_j^n}^{x_{j+1}^n} g(\rho(x,t),u(x,t))dxdt, \quad (10b)$$

where

$$\rho\left(x_j^n, t^{n+\frac{1}{2}}\right) \approx \tilde{\rho}^n(x_j^n) + \frac{\Delta t_n}{2}\rho_t(x_j^n, t_n), \quad (11a)$$

$$\mathrm{u}\,(x_j^n, t^{n+\frac{1}{2}}) \approx \tilde{u}^n(x_j^n) + \frac{\Delta t_n}{2}u_t(x_j^n, t_n), \quad (11b)$$

and from (5a) and (5b), we have $\tilde{\rho}^n(x_j^n) = \bar{\rho}_j^n$ and $\tilde{u}^n(x_j^n) = \bar{u}_j^n$.

The time derivatives ρ_t and u_t in (11a) and (11b) are respectively obtained from (3)

$$\rho_t(x_j^n, t^n) = -F_x, \quad u_t(x_j^n, t^n) = -G_x + g, \quad (12)$$

and the space derivatives F_x, G_x in (12) are computed using the minmod limiter.

2.2. Mesh redistribution

In this section, we briefly describe the second main part of our new method which is new mesh redistribution method. We steer mesh points by considering the

characteristic curves as a moving mesh equations. For the scalar conservation law:

$$\frac{\partial \rho(x,t)}{\partial t} + \frac{\partial F(\rho(x,t))}{\partial x} = g(x,t), \tag{13}$$

we are led to the following system of coupled ODEs:

$$\frac{dx}{dt} = \frac{\partial F}{\partial \rho} = v(\rho), \qquad \frac{d\rho}{dt} = g(x,t), \tag{14}$$

where the first equation determines the location of characteristic curves in time.
For the system of conservation laws:

$$\frac{\partial U}{\partial t} + A(U)\frac{\partial U}{\partial x} = G, \qquad x \in \mathbb{R},\ t > 0, \tag{15}$$

where $U = (\rho(x,t), u(x,t))^T$ and A, a 2×2 matrix, is the Jacobian of F in (1). Assume that the system is strictly hyperbolic, i.e., all eigenvalues of the matrix A are real, and the corresponding eigenvectors span $\mathbb{R}^2$.
The eigenvalues $v_1(U), v_2(U)$, of the matrix A are the characteristic speeds, i.e., the equations

$$\frac{dx}{dt} = v_1(U), \quad \frac{dx}{dt} = v_2(U), \tag{16}$$

are the characteristic curves equations.

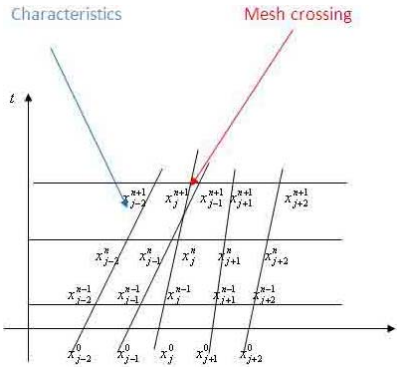

Fig. 1. Mesh trajectories and mesh crossing

In our new method, we move points using characteristic curves, i.e., x_j^{n-1}'s at t^{n-1} in Fig. 1 move to x_j^n's at t^n following characteristics.
In fact, we use the discretization of characteristic equation

$$\begin{cases} x_j^{n+1} = x_j^n + \Delta t_n v(U(x_j^n, t^n)), \\ x_0 = a, \qquad x_N = b, \end{cases} \tag{17}$$

where for system (15), v can be v_1 or v_2 or their average. We then couple this equation with equations (10a) and (10b).

If the characteristic curves intersect as it is shown in Fig. 1, then, $x_j^{n+1} < x_{j-1}^{n+1}$ at time $t = t^{n+1}$, and so mesh crossing will be produced. For this reason, we move these points by another strategy using the fact that two characteristics intersect when a shock wave is generated.

2.2.1. Shock Speed and Non-crossing Mesh

In the context of vehicle traffic, a shock wave is an abrupt change in traffic density. A shock wave will have a velocity of propagation. The shock velocity is like the velocity of density or traffic waves that is not related to the vehicle speed. When a shock wave is generated, characteristics intersect. It then represents a mathematical discontinuity (abrupt change) in ρ, u, or F.

Consider a segment $[x_1, x_2]$ of one-lane road, and suppose that the density of the traffic in this segment has a discontinuity at a point $\xi(t)$. We divide up the integral giving the number of vehicles N in this segment at the point ξ:

$$N = \int_{x_1}^{\xi} \rho(x,t)dx + \int_{\xi}^{x_2} \rho(x,t)dx. \tag{18}$$

Conservation of number gives

$$\begin{aligned} \frac{dN}{dt} &= F_{x_1} - F_{x_2} \\ &= \int_{x_1}^{\xi} \frac{\partial \rho}{\partial t}dx + \rho(\xi_-)\frac{d\xi}{dt} \\ &+ \int_{\xi}^{x_2} \frac{\partial \rho}{\partial t}dx - \rho(\xi_+)\frac{d\xi}{dt}. \end{aligned} \tag{19}$$

Using $\frac{\partial \rho}{\partial t} = -\frac{\partial F}{\partial x} = 0$, in the integrals and applying the fundamental theorem of calculus, we have

$$\begin{aligned} \frac{dN}{dt} &= F_{x_1} - F_{x_2} \\ &= -F(\rho(\xi_-)) + F_{x_1} + \rho(\xi_-)\frac{d\xi}{dt} \\ &+F(\rho(\xi_+)) - F_{x_2} + \rho(\xi_+)\frac{d\xi}{dt}. \end{aligned} \tag{20}$$

so we have

$$(\rho(\xi_+) - \rho(\xi_-))\frac{d\xi}{dt} = F(\rho(\xi_+)) - F(\rho(\xi_+)). \tag{21}$$

If the shock speed is $S = \frac{d\xi}{dt}$, this is sometimes written simply as $S[[\rho]] = [[F]]$, where $[[.]]$ represents the jump across the shock.

For a scalar conservation law, we can divide by $(\rho(\xi+) - \rho(\xi-)$ and obtain the shock speed:

$$S = \frac{F(\rho(\xi_+)) - F(\rho(\xi_-))}{\rho(\xi_+) - \rho(\xi_-)}. \tag{22}$$

In general $\rho(\xi_+, t)$ and $\rho(\xi_-, t)$, stands just to the right and the left of the shock, vary with time and the shock speed also varies.

For systems of equations, $\rho(\xi_+) - \rho(\xi_-)$ and $F(\rho(\xi_+)) - F(\rho(\xi_-))$ are both vectors while S is still a scalar. Now we cannot always solve for s to make (21) hold. Instead, only certain jumps $\rho(\xi_+) - \rho(\xi_-)$ are allowed, namely those for which the vectors $F(\rho(\xi_+)) - F(\rho(\xi_-))$ and $\rho(\xi_+) - \rho(\xi_-)$ are linearly dependent.

Now let us consider the situation whereby two characteristics intersect as Fig. 1 at time t^n to time t^{n+1}. When in general $x_j^{n+1} \le x_{j-1}^{n+1}$, we move points x_j^n, x_{j-1}^n using the following equation:

$$\frac{dx}{dt} = S, \tag{23}$$

or

$$\begin{cases} x_j^{n+1} = x_j^n + S\Delta t_n, \\ x_0 = a, \qquad x_N = b, \end{cases} \tag{24}$$

as can be seen in Fig. 2.

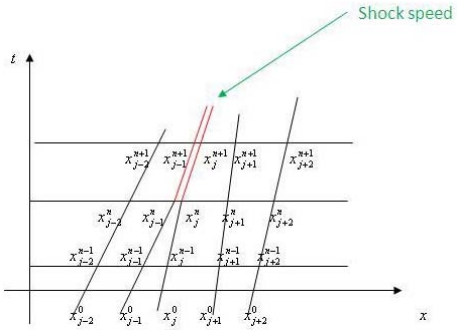

Fig. 2. New mesh trajectories

The basic idea of our algorithm can be summarized as follows:

Algorithm 1

Let $P = \emptyset$,

1. *(I)* Given a uniform mesh of the physical domain and mesh points $\{x_0^0, x_1^0, \ldots, x_N^0\}$. Then compute the grid values $\rho_j^{[0]}$ and $u_j^{[0]}$, $j = 1, \ldots, N-1$ based on the cell average for the initial $\rho(x,0)$, $u(x,0)$.

(II) Assume x_j^n, ρ_j^n and u_j^n were obtained.

2. Compute $\rho(x_{j+\frac{1}{2}}^n, t_{n+1})$ and $u(x_{j+\frac{1}{2}}^n, t_{n+1})$ based on non-oscillatory finite volume method,

(II) If $j \notin P$ then move grid x_j^n to x_j^{n+1} based on characteristics equation (17), else based on shock speed equation (24).

If $x_j^{n+1} \le x_{j-1}^{n+1}$, Move grids x_{j-1}^n, x_j^n to x_{j-1}^{n+1}, x_j^{n+1} based on shock speed equation (24), and $P = P \cup \{j-1, j\}$.

(III) Compute $x_{j+\frac{1}{2}}^{n+1} = \frac{x_j^{n+1} + x_{j+1}^{n+1}}{2}, j = 1, \ldots, \mathrm{N}-1.$

(Iv) Update numerical solution $\rho_{j+\frac{1}{2}}^{n+1}$ and $u_{j+\frac{1}{2}}^{n+1}$ on the new grids $\{x_{j+\frac{1}{2}}^{n+1}\}$.

3. If $t_{n+1} \le T$, then $\rho_{j+\frac{1}{2}}^{[0]} := \rho_{j+\frac{1}{2}}^{n+1}$,

$u_{j+\frac{1}{2}}^{[0]} := u_{j+\frac{1}{2}}^{n+1}$, $x_{j+\frac{1}{2}}^{[0]} := x_{j+\frac{1}{2}}^{n+1}$, and go to step 2.

Some remarks on step 2.

Vector P shows the points that move by the shock speed equation (24).

After obtaining the new grid $\{x_{j+\frac{1}{2}}^{n+1}\}$, we need to update ρ and u at these grid points (i.e. $\rho_{j+\frac{1}{2}}^{n+1}, u_{j+\frac{1}{2}}^{n+1}$). For this purpose, we use the formula obtained from the perturbation method (Tang and Tang, 2003). Numerical solutions are updated on the new grids $\{x_{j+\frac{1}{2}}^{n+1}\}$ (at the same time) using,

$$u_{j+\frac{1}{2}}^{n+1} = \beta_j u(x_{j+\frac{1}{2}}^n, t^{n+1}) - \gamma_j((\widehat{cu})_{j+1} - (\widehat{cu})_j), \qquad (25)$$

where

$$\gamma_j = (x_{j+1}^{n+1} - x_j^{n+1})^{-1}, \qquad \beta_j = \gamma_j.(x_{j+1}^n - x_j^n),$$

and

$$(\widehat{cu})_j = \frac{c_j}{2}(u_j^+ + u_j^-) - \frac{|c_j|}{2}(u_j^+ - u_j^-).$$

The c_j is defined by $c_j = x_j^n - x_j^{n+1}$, and

$$u_j^{\pm} = u_{j\pm\frac{1}{2}} + \frac{1}{2}(x_j - x_{j\pm1})\tilde{S}_{j\pm\frac{1}{2}},$$

where $\tilde{S}_{j\pm\frac{1}{2}}$ is an approximation of the slope u_x at $x_{j+\frac{1}{2}}$, and is

$$\tilde{S}_{j+\frac{1}{2}} = (sign(\tilde{S}_{j+\frac{1}{2}}^+) + sign(\tilde{S}_{j+\frac{1}{2}}^-)) \frac{|\tilde{S}_{j+\frac{1}{2}}^+ \tilde{S}_{j+\frac{1}{2}}^-|}{|\tilde{S}_{j+\frac{1}{2}}^+| + |\tilde{S}_{j+\frac{1}{2}}^-|},$$

with

$$\tilde{S}_{j+\frac{1}{2}}^+ = \frac{u_{j+\frac{3}{2}}^n - u_{j+\frac{1}{2}}^n}{x_{j+\frac{3}{2}} - x_{j+\frac{1}{2}}}, \quad \tilde{S}_{j+\frac{1}{2}}^- = \frac{u_{j+\frac{1}{2}}^n - u_{j-\frac{1}{2}}^n}{x_{j+\frac{1}{2}} - x_{j-\frac{1}{2}}}.$$

For more details see (Tang and Tang, 2003).

3. Numerical results

In this section, we illustrate the performance of the new moving mesh finite volume method.

Example 1. First, we test our adaptive mesh generation algorithm with the equation (1) from (Leveque, 2002). Let $g(x,t) = 0$ and the flux function $F(\rho(x,t)) = \rho U(\rho)$, and $U(\rho)$ varies linearly with ρ, i.e.

$$U(\rho) = u_{max}(1-\rho), \quad for \ 0 \le \rho \le 1.$$

At zero density (empty road) the speed is u_{max}, but decreases to zero as ρ approaches to 1. Then the flux function is defined:

$$F(\rho) = u_{max}\rho(1-\rho). \qquad (26)$$

We first suppose that at $t = 0$ the density on the road is given by

$$\rho(x,0) = 0.25 + 0.7e^{(-\beta x^2)}, \qquad (27)$$

with $\beta = 0.01, u_{max} = 1$. Since $v(\rho) = u_{max}(1-2\rho)$, the mesh equation should be:

$$\frac{dx}{dt} = u_{max}(1-2\rho).$$

Figure 3(a) shows the numerical solutions at time $t = 25$ computed in (Leveque, (2002) by Clawpack and the new proposed scheme. A very high quality of the computed solution can be observed, especially at the contact discontinuity. Figure 4 shows the close-up view of the Fig. 3(c).

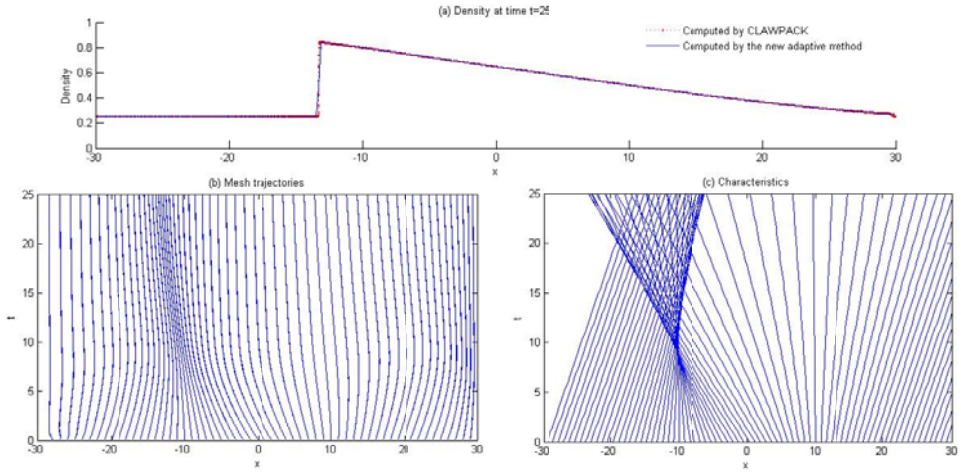

Fig. 3. Example 1. Top: Computed solution at t=25, with N=120 mesh points by new adaptive method and Clawpack. Bottom: The corresponding characteristics and the mesh trajectories

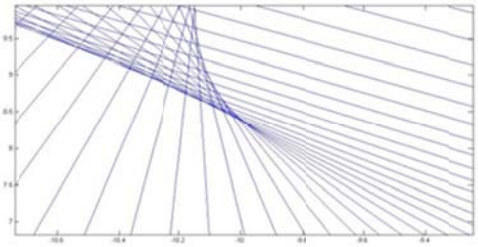

Fig. 4. Close-up view of the shock formation in Example 1

Let T^* signify the critical time in which for the first time, characteristic curves intersect. T^* is given by Godlewski and Raviart (1996),

$$T^* = -\frac{1}{\min(\alpha, 0)}, \quad \alpha = \min_{y\in\mathbb{R}} \frac{d}{dy} v(u_0(y)).$$

In this example, $\alpha = -0.1201$ and as can be seen in Fig. 4, the characteristic curves intersect at $T^* = 8.3264$ when shock starts to form. The shock velocity is given by $[1 - (\rho(\xi_+) + \rho(\xi_-))]$ so mesh
speed at shock region is,

$$\frac{dx_i^n}{dt} = [1 - (\rho(x_{i+1}^n, t_n) + \rho(x_{i-1}^n, t_n))].$$

Example 2. For the second example, we consider one more simulation for special cases corresponding to previous traffic problem in which the initial data is the following piecewise constant function:

$$\rho(x,0) = \begin{cases} 1, & 0 \le x \le 10, \\ 0.25, & -40 \le x < 0. \end{cases}$$

Figure 5 can be interpreted as cars approaching a traffic jam, or a line of cars waiting for a traffic light to change. Note that the solution to the traffic problem may consist of a shock wave as in Fig. 5.

Example 3. For the last example, we consider the system (2), with the following initial and boundary conditions

$$\rho(x,0) = \begin{cases} \rho(x_0,t) = 0.04(veh/m), & 0 < x < 10, \\ \rho(x_N,t) = 0.18(veh/m), & 10 \le x < 20. \end{cases}$$

$$u(x,0) = \begin{cases} u(x_0,t) = u_e(\rho(x_0,t)), & 0 < x < 10, \\ u(x_N,t) = u_e(\rho(x_N,t)), & 10 \le x < 20. \end{cases}$$

The equilibrium speed-density relationship developed in (Del Castillo and Benitez, 1995) is applied

$$u_e = u_f[1 - exp(1 - exp(\frac{c_m}{u_f}(\frac{\rho_m}{\rho} - 1)))],$$

where u_f is the free-flow speed; ρ_m is the maximum density and c_m is the kinematic wave speed under the jam density. The test road section is 20 km long. Parameter values used are as follows (Jiang et al, 2002):

$$u_f = 30 \ \frac{m}{s}, \quad \rho_m = 0.2 \ \frac{veh}{m},$$
$$T = 10s, \quad c_m = c_0 = 11 \ m/s.$$

The model can be written as

$$\begin{pmatrix} \rho \\ u \end{pmatrix}_t + \begin{pmatrix} \rho u \\ \frac{u^2}{2} - c_0 u \end{pmatrix}_x = \begin{pmatrix} 0 \\ \frac{u_e - u}{T} \end{pmatrix}. \tag{28}$$

In comparison with (15), we have

$$U = \begin{bmatrix} \rho \\ u \end{bmatrix}, \quad [A] = \begin{bmatrix} u & \rho \\ 0 & u - c_0 \end{bmatrix},$$

$$G = \begin{bmatrix} 0 \\ \frac{u_e - u}{T} \end{bmatrix} \quad (29)$$

The eigenvalues of the matrix A are $\lambda_1 = \mathrm{u}$, $\lambda_2 = u - c_0$.
Thus the characteristics curves are

$$\frac{dx}{dt} = \lambda_1 = u, \quad \frac{dx}{dt} = \lambda_2 = u - c_0. \quad (30)$$

The shock speed is

$$\frac{dx}{dt} = \frac{F_e(\rho_1) - F_e(\rho_2)}{\rho_1 - \rho_2}, \quad (31)$$

where $F_e = u_e \rho$ and ρ_1 and ρ_2 are the amount of ρ at $X = -\infty$ and $X = +\infty$ respectively.

The results at time $t = 10$ under the characteristic curves $\frac{dx}{dt} = \lambda_1 = u$ (called 1^{st}-characteristic), $\frac{dx}{dt} = \lambda_2 = u - c$ (called2^{nd}-characteristic), and also $\frac{dx}{dt} = \frac{1}{2}(\lambda_1 + \lambda_2)$ (called the average of 1^{st}- and 2^{nd}-characteristics), are shown in Figs. 6(a), 6(b). Figures 6(c), 6(d) and 6(e) show the corresponding mesh trajectories with different mesh speed based on 1^{st}- and 2^{nd}- and the average of both characteristic curves, respectively.

4. Characteristic curves and moving mesh method

It is useful to compare the method introduced in the previous sections with the moving mesh method that has been used in (Soheili et al, 2013).

Example 4. We apply the moving mesh method introduced in (Soheili et al, 2013) for Example 3. In this case, the mesh equation is given by modified $MMPDE5$:

$$\frac{\partial x}{\partial t} = \frac{1}{\tau M} \frac{\partial}{\partial \xi}\left(M \frac{\partial x}{\partial \xi}\right), \quad (32)$$

where M is the arc-length monitor function:

$$M = (1 + \alpha \nabla U (\nabla U)^T)^{\frac{1}{2}}, \quad (33)$$

where U is defined by (28). Then we combine the moving mesh method and new adaptive method together. One way to do this is to compute the mesh based on modified MMPDE5 and based on the characteristic curves first and then generate the new one using the average of them.

Figure 7 shows the mesh generated using (32), (30) (and (31)) and using a combination of them. As can be seen, the numerical results are almost the same and since the CPU time in the introduced method is much less than the CPU time in MMPDE method and, on the other hand, in situations when time is an important factor, the new method would be more useful.

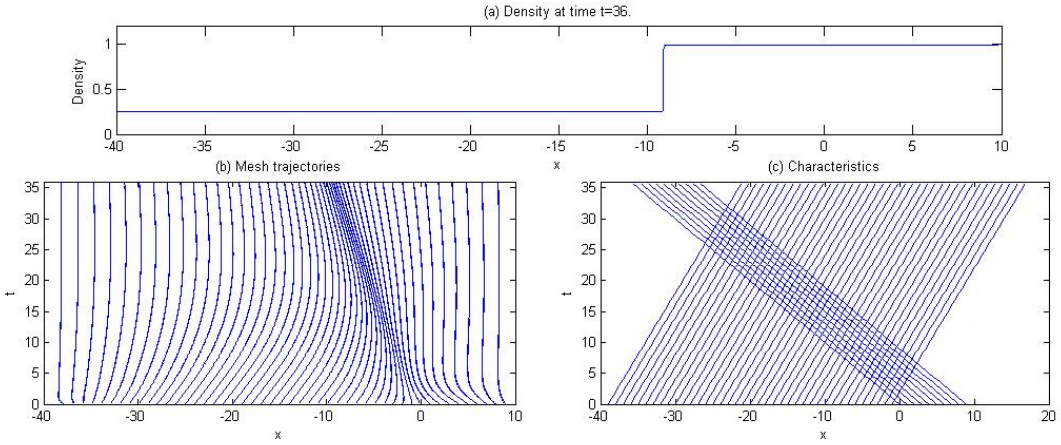

Fig. 5. Example 2. Top: Computed solution at t=36, with N=100 mesh points. Bottom: corresponding characteristics and mesh trajectories

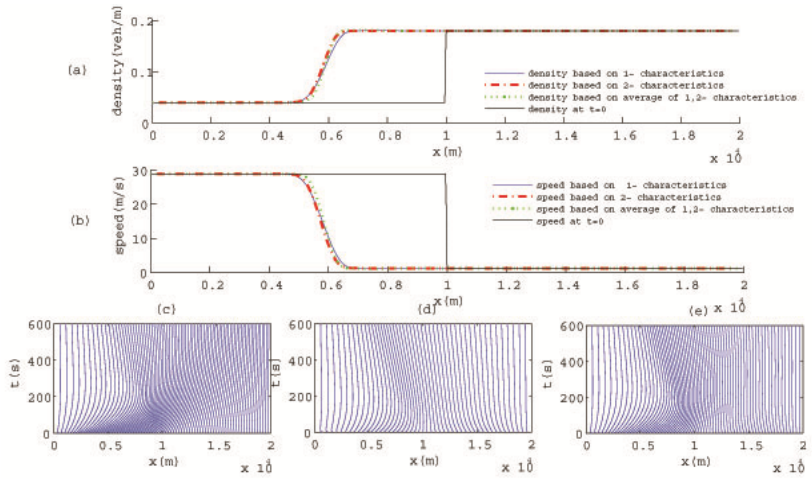

Fig. 6. Example 3. (a), (b): Computed density and speed at $t = 600$s with different mesh speed. (c), (d) and (e): The mesh trajectories corresponded to the 1 and 2 and average of 1, 2 -characteristics respectively

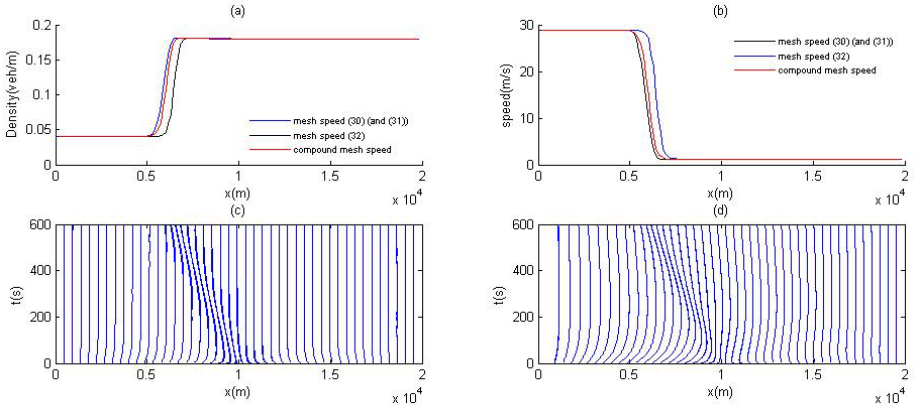

Fig. 7. Example 2. (a), (b): Computed solution at $t = 600$s with different mesh speeds. (c), (d): The mesh trajectories with mesh speed based on moving mesh method and combined method respectively

5. Conclusions

It is important to apply proper numerical treatment to the macroscopic models in the simulation of traffic flow. In the present paper, we have attempted to present a new method with mesh selection based on the characteristics and shock speed equations, for solving macroscopic traffic flow models. The accuracy of our results are derived from combining the high resolution scheme for the physical equations with a new mesh generation method that uses characteristics.

The application of this method for traffic flow problems demonstrates that the new method is an effective scheme to obtain sharp resolution of traffic flow features with large gradients such as shock waves. The method is suitable for any nonlinear system of hyperbolic PDEs based on conservation laws, where numerical conservation is guaranteed.

Some numerical experiments have shown the effectiveness of our approximation. The comparison of the MMPDE5 and our new mesh generation method has been presented too.

Acknowledgment

This research was in part supported by a grant from the Center of excellence on Modelling and Control Systems, (CEMCS).

References

Del Castillo, J. M., & Benitez, F. G. (1995). On functional form of the speed–density relationship I: general theory, II: empirical investigation. *Transportation Research Part B: Methodological B*, 29(5), 373–406.

Godlewski, E., & Raviart, P. A. (1996). Numerical approximation of hyperbolic system of conservation laws. *Applied Mathematical Sciences*, Springer.

Huang, W., Ren, Y., & Russell, R. D. (1994). Moving mesh partial differential equations (MMPDEs) based

upon the equidistribution principle. *SIAM Journal on Numerical Analysis*, 31(3), 709–730.

Huang, W., & Russell, R. D. (2011). *Adaptive Moving Mesh Method*. New York, Springer.

Jiang, R., Wu, Q., & Zhu, Z. (2002). A new continuum model for traffic flow and numerical tests. *Transportation Research Part B*, 36, 405–419.

Leveque, R. (2002). Finite volume Methods for hyperbolic problems. *Cambridge University Press*.

Lighthill, M. J., & Whitham, G. B. (1955). On kinematic waves: II. a theory of traffic flow on long crowded roads, *Proceedings Royal Society, London, Series A* 229(1178), 317–345.

Nessyahu, H., & Tadmor, E. (1990). Non-oscillatory Central Differencing for Hyperbolic Conservation Laws. *Journal of Computational Physics*, 87(2), 408–463.

Payne, H. J. (1971). Models of freeway traffic and control. *Simulation Councils Proceedings Series: Mathematical Models of Public Systems*, 1(1), 51–61.

Richards, P. I. (1956). Shock waves on highways. *Operations Research*, 4(1), 42–51.

Soheili, A. R., Kerayechian, A., & Davoodi, N. (2012). Adaptive numerical method for Burgers-type nonlinear equations. *Applied Mathematics and Computation*, 219, 3486–3495.

Soheili, A. R., Kerayechian, A., Tareghian, H. R., & Davoodi, N. (2013). Adaptive Numerical Simulation of Traffic Flow Density. *Computers and Mathematics with Applications*, 66, 227–237.

Stockie, J. M., Mackenzie, J. A., & Russell, R.D. (2001). A moving mesh method for one-dimensional hyperbolic conservation laws. *SIAM Journal on Scientific Computing*, 22(5), 1791–1813.

Tang, H., & Tang, T. (2003). Adaptive mesh methods for one- and two-dimensional hyperbolic conservation laws. *SIAM Journal on Numerical Analysis*, 41(2), 487–515.

Tang, T. Q., Huang, H. J., & Shang, H. Y. (2010). A new macro model for traffic flow with the consideration of the driver's forecast effects. *Physics letters A*, 374, 1668–1672.

Zhang, H. M. (1998). A theory of a nonequilibrium traffic flow, *Transportation Research Part B*, 32, 385–498.